



# Comparative analysis of light trapping GaN nanohole and nanorod arrays for UV detectors

Xingyue Zhangyang · Lei Liu  · Zhisheng Lv · Feifei Lu · Jian Tian

Received: 9 March 2020 / Accepted: 3 August 2020 / Published online: 11 August 2020  
© Springer Nature B.V. 2020

**Abstract** In this paper, based on the excellent light trapping performance of the nanostructure, the structure of the electron emission layer of the ultraviolet detector is optimized. In this paper, simulation models of gallium nitride (GaN) nanohole arrays and nanorod arrays are designed by COMSOL Multiphysics software, which is based on the finite element method (FEM). In order to optimize the geometric parameters of GaN nanohole and nanorod arrays, and understand the influence of polarized light on them, the light absorption performance in the ultraviolet (UV) band has been fully analyzed. We found that when the lattice constant ranges from 200 to 500 nm, the GaN nanohole array and the GaN nanorod array have extreme absorptivity. And when the incident light has an inclination of 20°, the light trapping performance of the nanohole array can be further improved. GaN nanostructures with high light trapping capabilities will help improve the photoelectric emission efficiency of GaN photocathode and provide design reference for UV detectors with excellent performance.

**Keywords** GaN nanostructure · Photocathode · FEM · Light trapping · COMSOL multiphysics · Modeling and simulation

## Introduction

In the solar radiant energy, the ultraviolet band accounts for about 7%, and the ozone layer has a strong absorption effect on the light in the 200–400 nm band. Ultraviolet detectors operating in the ultraviolet range have been greatly used in the context of detection. The image intensifier is a vacuum-type GaN ultraviolet detector and focuses on weak UV signal detection and imaging systems; it has the advantages of fast response, stable performance, low noise, and high gain.

In recent years, there are many studies about the optical properties of various of nanostructures, such as nanowire (Garnett and Yang 2008, Garnett and Yang 2010, Cao et al. 2010, Fang et al. 2014, Li et al. 2015, Wu et al. 2017, Xu et al. 2017, Wang et al., 2017a, b), nanocone (Xu et al. 2016), nano-hemisphere (Kang and Fang 2014), truncated nanocone (Kim et al. 2018), pyramid (Tan et al. 2017), motheye (Makableh et al. 2018), nanohole (Han and Chen 2010, Peng et al. 2010, Adib et al. 2012, Fang et al. 2014, Chen et al. 2014, Hong et al. 2014, Wang et al. 2016, Wang et al. 2017a, 2017b, Deng et al. 2018, Fu et al. 2018), and nano-cone-hole (Du et al. 2011). The main materials of those nanostructures are silicon, silicon nitride, silicon carbide, gallium arsenide, or gallium nitride. GaN has a low electron affinity and stable physical and chemical properties, so it is widely used as a photocathode material (Chung and Gershenson 1992, Yoshida et al. 2001, Look et al. 2002, Fu et al. 2010, Cheng et al. 2015). In previous studies, nanostructures have been found to have superior optical properties compared with thin film

---

X. Zhangyang · L. Liu (✉) · Z. Lv · F. Lu · J. Tian  
Department of Optoelectronic Technology, School of Electronic and Optical Engineering, Nanjing University of Science and Technology, Nanjing 210094, China  
e-mail: liu1133\_cn@sina.com.cn

structures, such as antireflection and enhanced light absorption. The work of Hao Lin et al. shows that the optical properties of nanostructures are mainly affected by geometric factors such as structural spacing, material filling ratio, and aspect ratio (Lin et al. 2014). Studies in Fang X et al. have shown that incident light with a range of angles enables nanostructures to achieve higher absorption performance (Fang et al. 2014). Therefore, in the work of this paper, GaN is the nanostructured material. We used COMSOL Multiphysics Business Package to simulate the different diameters and lattice constants of nanohole arrays and nanorod arrays. We studied the absorption differences of the two nanostructures under the same parameters; then, we changed the angle of incident light to study the effect of different polarized light on the absorption performance of nanostructures. This study provides a possible way to improve the photoelectric performance of the vacuum type UV detector.

## Models and method

In this paper, COMSOL Multiphysics software is used to calculate the optical performance of nanostructures. The schematic diagram of structure of nanohole arrays

and nanorod arrays is shown in Fig. 1a and b. A cube region is used as the simulation region of the nanostructure arrays. The simulation regions of nanohole arrays and nanorod arrays are shown in Fig. 1c and d, respectively. To reduce the workload and complexity of calculation, the simulation region is set as a repeating simulation unit by defined “periodic boundary conditions.” Nanostructure arrays can be achieved by setting the two opposite sides of the cube to the periodic boundary condition. In order to simulate the propagation of incident light in the simulation region in a real scene, perfect matching layer (PML) with thickness of 200 nm is defined at the top and bottom of the simulation region. By using the PMLs, it is possible to eliminate unwanted reflections in the simulation region and interference caused by reflected light. The  $S$  parameter is used to calculate the reflection and transmission of the simulation model, which is obtained by setting the two boundaries immediately adjacent to the PMLs as “port.” Absorption is calculated by Eq. (1):

$$A(\lambda) = 1 - R(\lambda) - T(\lambda) \quad (1)$$

where  $A(\lambda)$  is the absorption of the simulation models,  $R(\lambda)$  is the reflection calculated by port S1, and  $T(\lambda)$  is the reflection calculated by port S2. The polarized light is implemented by setting interior port as transverse

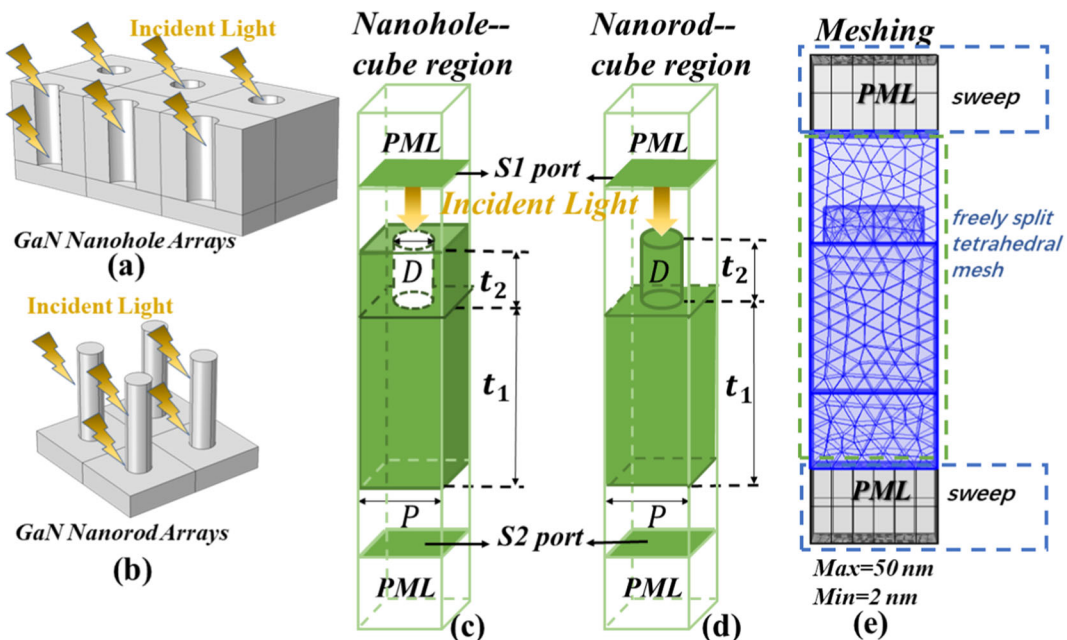


**Fig. 1** Schematic diagram of **a** GaN nanohole arrays and **b** GaN nanorod arrays. Simulation region structure of **c** nanohole and **d** nanorod in COMSOL. **e** Meshing settings in the simulation region

electric or magnetic wave (TM/ TE) field source and setting the port as a “periodic port.” Vacuum regions with a thickness of 200 nm are also disposed above and below the nanostructures. We defined the nanohole arrays and nanorod arrays with a thin film structure of thickness  $t_1$ ; the structure of nanoholes and nanorods with a thickness of  $t_2$  is constructed on the basis of thin film, where  $t_1$  is 400 nm,  $t_2$  is 100 nm,  $D$  is the diameter of nanohole and nanorod, and  $P$  is the lattice constant of the nanostructures. As shown in Fig. 1e, which is schematic diagram of meshing, the PMLs are set to “sweep” and the rest of the simulation region is set to the “freely split tetrahedral mesh.” For this physics interface, the maximum grid cell size is preferably less than 1/8 of the wavelength. The incident light wavelength range of this simulation model is 200 to 400 nm, so the maximum cell size is 50 nm and the minimum cell size is 2 nm. All simulation models use the same grid cell size to maintain computational rigor. The refractive index and extinction coefficient used in the model in this paper are from the literature (Antoine-Vincent et al. 2003).

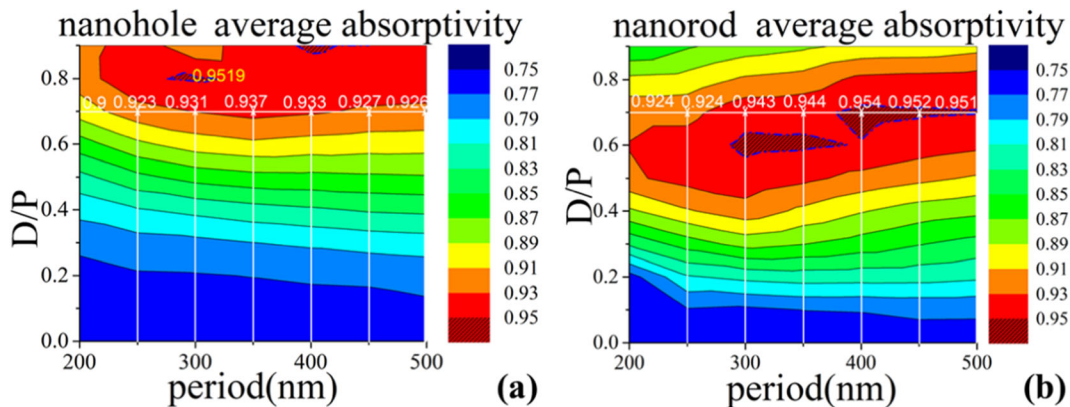
**Results and discussion**

Figure 2 shows the relationship between the average absorptivity and lattice constant and  $D/P$  of nanohole arrays and nanorod arrays. The simulation calculation is performed under the TM field source. The lattice constant varies from 200 to 500 nm, the interval is 50 nm, and the  $D/P$  is from 0.1 to 0.9. In the nanohole arrays, it can achieve absorptivity of 0.93 when it is in the range of 0.7 to 0.9, while in the nanorod arrays 0.93 can be

obtained in the range of  $D/P$  of 0.5 to 0.7. For the nanohole array, the lattice constant for obtaining the optimal absorptivity value of 0.9519 is 300 nm, and the  $D/P$  is 0.8. The parameter for the nanorod array to obtain the optimal absorptivity of 0.954 is  $P = 400$  nm,  $D/P = 0.7$ . The results show that the average absorptivity of GaN nanorod array is only 0.0021 higher than that of GaN nanohole array. Therefore, in order to study the different effects of the lattice constant on the light trapping performance of the nanohole array and the nanorod array. The following is comparative analysis of the difference in absorptivity spectra between nanohole and nanorod arrays at  $D/P = 0.7$ , where nanorod array can obtain extreme value of the average absorptivity.

The effect of lattice constants

Figure 3a shows the absorptivity spectra of nanohole array with fixed  $D/P$  of 0.7 and different lattice constants. It is clear that the increase of the lattice constant causes the absorptivity peak when  $P$  is in the range of 200 to 400 nm move to long-wave region. But when  $P$  is in the range of 400–500 nm, the peak of the absorptivity is concentrated around the wavelength of 360 nm. Similarly, in the process of expanding the lattice constant, the region of reduced absorptivity also expands to the long-wave region, which results in an extreme value of average absorptivity at  $P = 350$  nm as shown in Fig. 2a. Explained from the perspective of wave optics, when the wavelength of light matches the lattice constant of the nanohole array, the incident light is more effectively scattered around the nanopore structure, prolonging the optical path and enhancing light absorption. As shown



**Fig. 2** Average absorptivity with lattice constant and  $D/P$  changed of **a** nanohole arrays **b** nanorod arrays

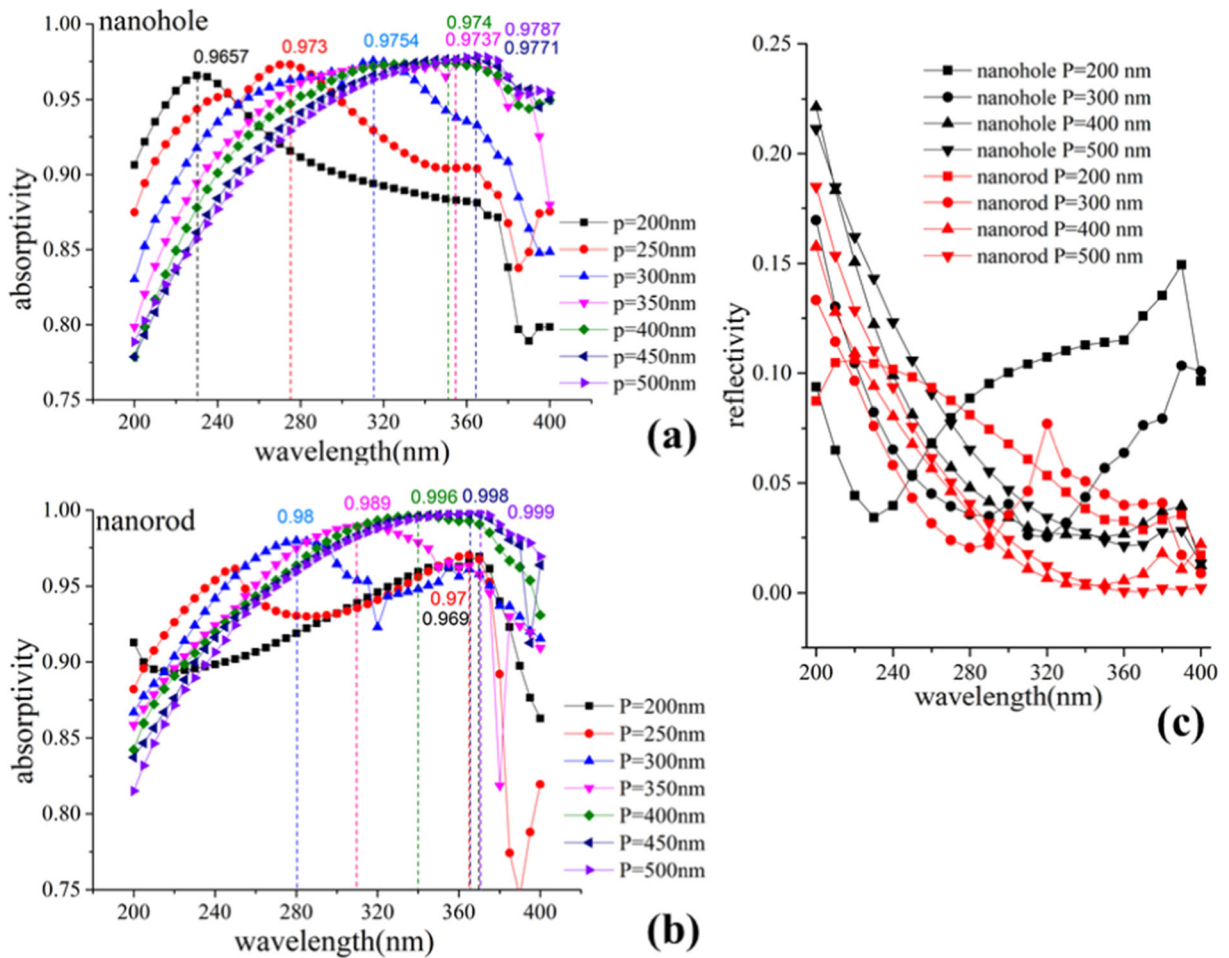


**Fig. 3** Absorptivity spectrum with a fixed D/P at 0.7 and different lattice constants of **a** nanohole arrays and **b** nanorod arrays. **c** Reflectivity spectrum of nanohole and nanorod arrays

in Fig. 3c, the reflection of the nanostructure in the short-wave region with P of 200 to 400 nm is suppressed, and in the long-wave region, when P is 400 to 500 nm, the reflection of the nanostructure is suppressed. Finally, the enhancement of light trapping capacity of the GaN nanohole array can be attributed to the suppression of reflection. Figure 3b shows the absorptivity spectra of nanorod arrays with fixed D/P of 0.7 and different P; the increase of the lattice constant causes the absorption peak move to the long-wave region when P is in the range of 200–500 nm. There are two absorptivity peaks when P is in the range of 200 to 300 nm. The absorptivity peak of the short-wave region moves toward the long-wave region under the influence of the increase of the lattice constant, much like the variation of the nanohole array. However, the absorptivity peak of the short-wave region of the nanorod array

is gradually increasing while moving. The absorption peak of the long-wave region of the nanorod array did not change under the influence of the increase of the lattice constant. When the lattice constant increased to 500 nm, the original absorption peak of the long-wave region is replaced by a gradually increasing new absorption peak, which is moved from the short-wavelength region. As such, the enhancement of nanorod array absorption can be attributed to inhibition of reflection. Comparing Fig. 3a and b, it can be seen that in the long-wave region, when P is larger than 400 nm, both structures can obtain high light trapping ability.

The effect of diameter

In order to analyze the effect of the diameter on the light trapping performance of the nanohole array and the

nanorod array, the lattice constant is fixed at 300 nm, and the average absorptivity extreme value of the nanohole array can be obtained when  $D/P = 0.8$ . Therefore, to highlight the difference between the two, the absorptivity spectra of  $D/P = 0.6$  and  $0.8$  are selected for analysis, which are shown in Fig. 4a on the premise that the lattice constant is fixed at 300 nm. The red lines are absorptivity spectrum with  $D/P$  of 0.6, and the absorptivity of the nanorod arrays is over that of nanohole arrays. The reason can be found in Fig. 4b and c. The transmission difference between the two nanostructures is negligible, but the reflectivity of the nanohole is significantly harmful. Shown in Fig. 4d is schematic of the structure of horizontal sections of nanostructures. When  $D/P$  is 0.6, the nanohole structure on the horizontal section has a wider area covered by GaN, so that the top side of the nanohole array is closer to the thin film structure. Conversely, in a horizontal cross section, the arrangement of GaN nanorod structures is sparser, so that normal incident light is not easily reflected. In Fig.

4a, the blue lines indicate the absorptivity spectrum with  $D/P$  of 0.8, and the absorptivity of the nanohole array is higher than that of the nanorod array, because the reflectivity of the nanohole array is suppressed. As seen in the schematic diagram of the structure in Fig. 4d, the diameter of nanorod becomes larger so that the nanorod array becomes dense, resulting in an increase in reflectivity. Conversely, the diameter of nanohole becomes larger so that incident light is more likely to sink into the structure of the nanohole, thus enhancing absorptivity.

Figure 5 shows the electric field distribution schematic of the nanohole array and the nanorod array at the wavelength of 300 nm. The geometric outline of the nanohole and nanorods is shown in the dashed box. The electric field distribution of the  $x$ - $y$  plane shown in the Fig. 5 is obtained at the junction of the nanostructure and the thin film. Light is well coupled into the nanostructures in the nanohole array. And when  $D/P$  is changed from 0.6 to 0.8, light continue to be coupled into the thin film, so absorptivity is enhanced. In the

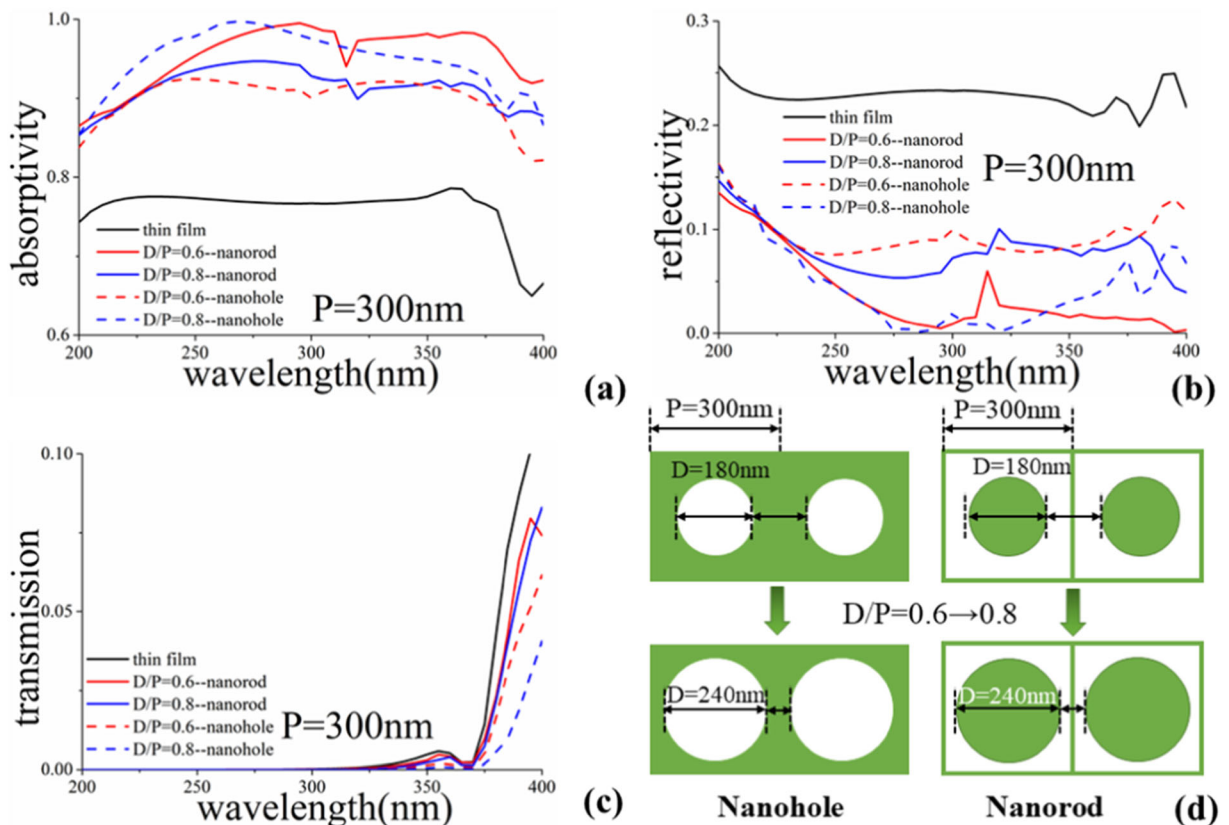


**Fig. 4** a Absorptivity, b reflectivity, and c transmission spectrum of nanohole arrays and nanorod arrays with fixed  $P$  of 300 nm and different  $D/P$ . d Structure diagram of horizontal cross section of nanohole arrays and nanorod arrays

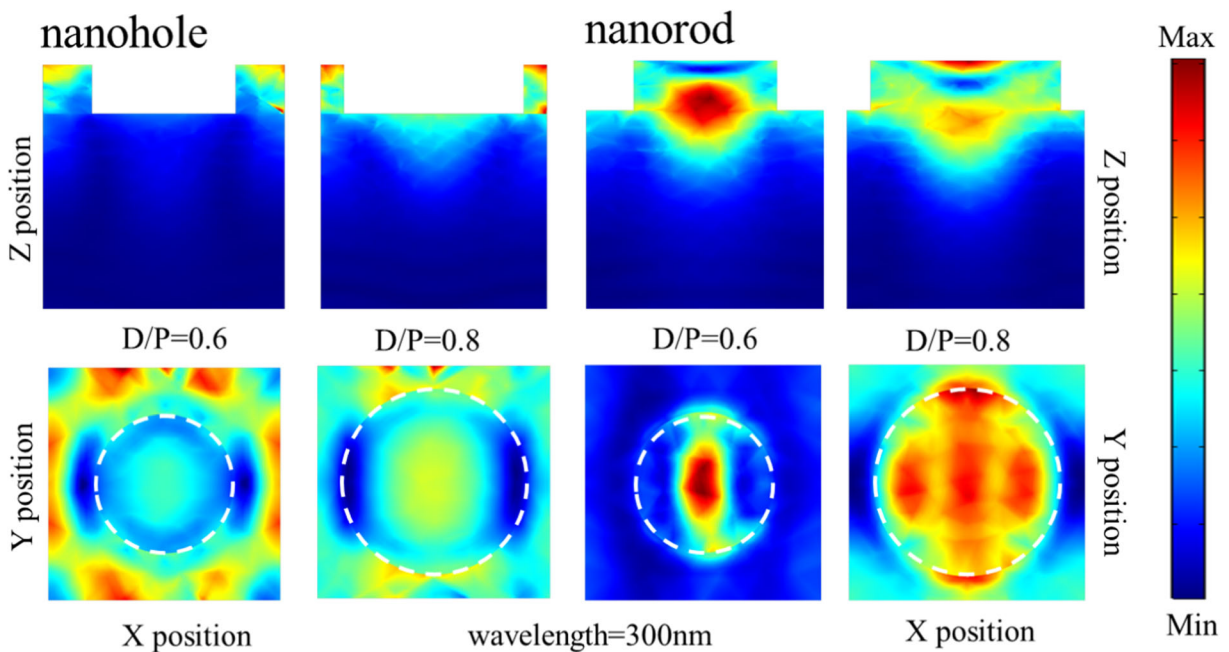


**Fig. 5** Schematic diagram of electric field distribution of nanohole arrays and nanorod arrays at the wavelength of 300 nm

nanorod array, light is coupled into the rod and directed into the thin film through the nanostructures. When  $D/P$  is changed from 0.6 to 0.8, the strength of the coupling is weakened, so the absorptivity is also weakened. The phenomenon of light coupling exhibited in the electric field distribution can prove the numerical analysis in the paper. Therefore, in the case where the lattice constant and diameter have extreme effects on the light absorption performance of nanostructures, the GaN nanohole array and GaN nanorod array can obtain the optimal results within the current parameter value range.

#### The effect of polarization and incident angle

Figure 6a and b shows the schematic diagram of TE, TM polarized light incident on nanohole array and nanorod array, where  $\alpha$  is the incident angle of polarized light. The electric field component of the TE polarized light is parallel to the  $y$ -axis, and the electric field component of the TM polarized light is in the  $xz$  plane. The absorptivity of the nanohole array and the nanorod array varies with the incident light angle  $\alpha$  as shown in Fig. 6c and d. The red and blue lines represent the average absorptivity of the nanostructures under TE polarized incident light and TM polarized incident light, respectively. The black line indicates the mixed

polarized incident light, which is the result of the arithmetic mean of absorption under the TE and TM polarized light. The overall absorptivity trend decreases as the incident angle of the TE polarized light increases. However, the absorptivity curve of TM polarized incident light is not monotonic. Under mixed polarized incident light, the two structures are capable of maintaining high absorptivity over a range of incident angles and higher than absorptivity at normal incidence. The nanohole array can increase absorptivity over a range of incident angles from 0 to 20°. Nanorod array can increase absorptivity over a range of incident angles from 0 to 40°. This means that the nanostructures should be tilted at a small angle to achieve higher absorptivity.

The absorptivity enhancement at small angle incidence is due to parallel interface refractivity. If the Bloch mode is completely parallel to the interface, it will not be able to excite resonance due to its infinite quality factor. Instead, the modal must be slightly offset from the parallel direction of the interface to produce a very strong resonance. The incident at a small angle satisfies the above conditions. The Fresnel formula can be used to explain the difference in absorptivity caused by different polarized light at large angles of incidence. When light interacts with the interface at different angles of incidence, the proportion of incident energy entering

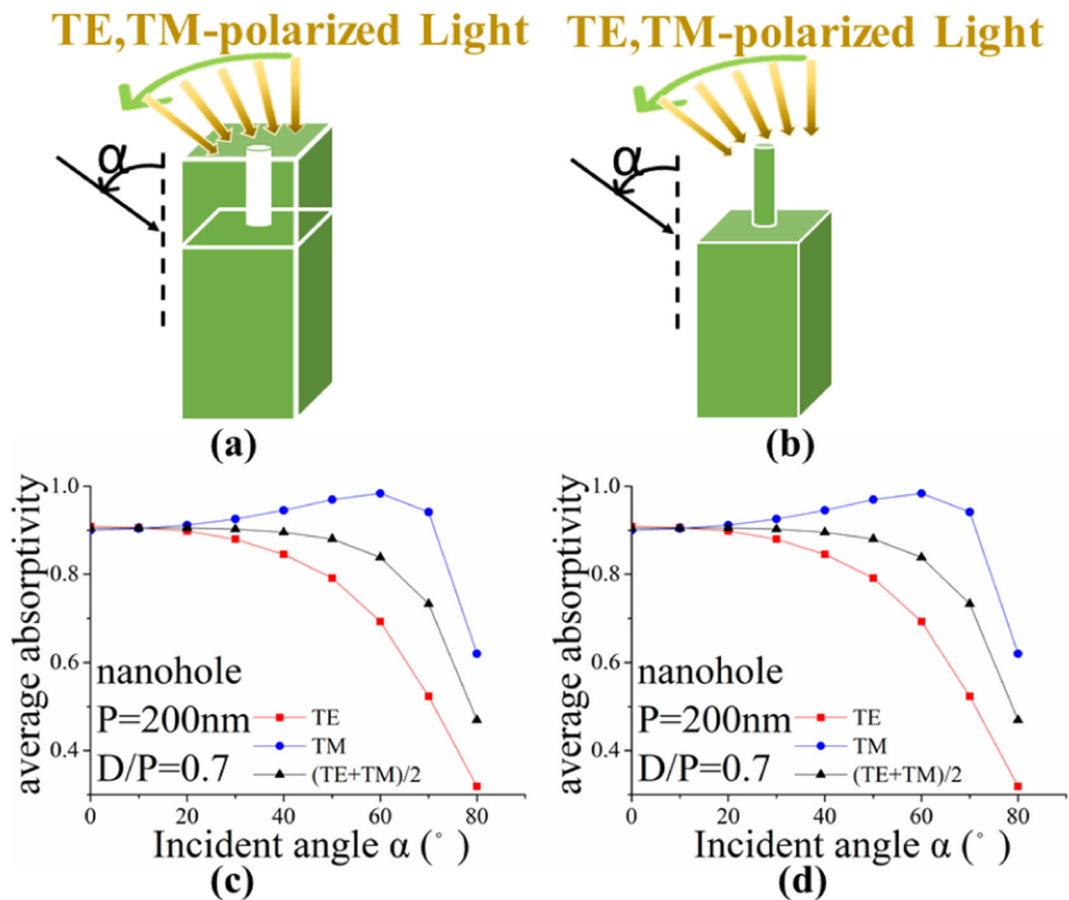


**Fig. 6** Schematic diagram of oblique incident light on **a** nanohole array and **b** nanorod array, and average absorptivity of **c** nanohole arrays and **d** nanorod array various with incident angle  $\alpha$

the transmitted medium is determined by the Fresnel formula. The transmission expressions for the two polarization directions are expressed by Eqs. (2) and (3):

$$T_{TE} = 1 - \frac{\sin^2(\alpha - \theta)}{\sin^2(\alpha + \theta)} \tag{2}$$

$$T_{TM} = 1 - \frac{\tan^2(\alpha - \theta)}{\tan^2(\alpha + \theta)} \tag{3}$$

where  $\alpha$  and  $\theta$  are the incident angle and the transmission angle and  $T_{TE}$  and  $T_{TM}$  are transmissivity. The transmissivity calculated by equations is different from the transmission obtained from COMSOL Multiphysics software, which is normalized light energy received by port S2. The transmissivity in Eqs. (2) and (3) is 1 subtract reflectivity; it is equal to the absorptivity plus transmission in the simulation results. The transmitted angle can be determined according to the law of refraction, and the law of refraction is as shown in Eq. (4):

$$n_1 \sin \alpha = n_2 \sin \theta \tag{4}$$

where  $n_1$  is the refractive index of the incident medium and  $n_2$  is the refractive index of the transmitted medium. In the simulation model of this paper, the incident medium is air and the transmitted medium is GaN nanostructure. The refractive index of the nanostructure cannot use the refractive index of GaN under the thin film structure. However, the effective medium refractive index of the nanostructures needs to be calculated according to the mathematical model proposed by Maxwell-Garnett. The effective refractive index  $n_{\text{eff}}$  is determined by the formula (5) Maxwell-Garnett model.

$$\left[ \frac{n_{\text{eff}}^2 - n_1^2}{n_{\text{eff}}^2 + 2n_1^2} \right]^2 = (1-f) \left[ \frac{n_2^2 - n_1^2}{n_2^2 + 2n_1^2} \right]^2 \tag{5}$$

This formula is built on the assumption that the medium  $n_2$  is surrounded by the medium  $n_1$ .  $n_1$  is the refractive index of air,  $n_2$  is the refractive index of the

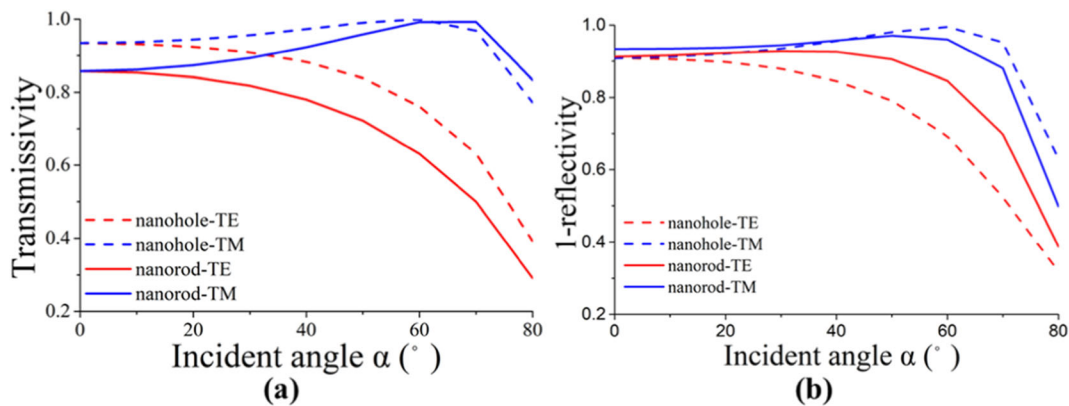


**Fig. 7** **a** Transmissivity curve of nanohole array and nanorod array calculated by Eqs. (2) and (3) with increasing incident angle of polarized light. **b** Transmissivity (1-reflectivity) curve calculated by COMSOL Multiphysics

GaN film, and  $f$  is the filling ratio of the GaN material in the nanostructure. The nanohole array has a D/P of 0.7, and  $f$  is 0.923. The nanorod array has a D/P of 0.7, and  $f$  is 0.877. The refractive index of the GaN material is in the wavelength of 200–400 nm. The  $n_{\text{eff}}$  of the nanohole array is 1.689, and the  $n_{\text{eff}}$  of the nanorod array is 2.212.

The transmissivity of the nanohole array and the nanorod array under the incidence of two polarized lights is illustrated in Fig. 7. What is in Fig. 7a is transmissivity calculated by Eqs. (2) and (3), and in Fig. 7b is transmissivity calculated by COMSOL Multiphysics software, which is equal to 1 subtract reflectivity. Comparing Fig. 7a and b, it is clear that the curve trends are very similar. Therefore, by using Fresnel formula and effective medium refractive index model, it is possible to explain the phenomenon that the absorptivity changes with the angle of incident light in the COMSOL simulation results. It can be seen in Fig. 7a that the transmissivity of the TE polarized incident light keeps decreasing, while the transmissivity of the TM polarized incident is non-monotonic with the increase of incident light in both nanostructures. Therefore, as the incident angle of the TE polarized light increases, less energy enters the GaN nanostructure, and the absorptivity is correspondingly weakened. Conversely, over a range of incident angles, as the incident angle of the TM polarized light increases, more energy enters the nanostructure, resulting in enhanced absorptivity.

## Conclusion

In the work of this paper, we used COMSOL Multiphysics Business Package to simulate the GaN

nanohole arrays and nanorod arrays. Our goal is to compare and analyze the absorption performance of two nanostructures. Firstly, we fixed the D/P of the nanostructures. In the process of increasing the lattice constant, we found that the absorptivity peak of the nanostructures appeared to move to the long-wave region. After the lattice constant is increased to 400 nm, both nanostructures are able to obtain higher absorption capacity in the near ultraviolet range. Secondly, we fixed the lattice constant and compared the optical properties of two nanostructures at different D/P. We found that the GaN nanohole array has a stronger ability to trap light when D/P is 0.8, and this can be attributed to the nanohole structure having stronger anti-reflection ability. Moreover, when D/P is larger than 0.8, the nanohole array will use less material than the nanorod array. Finally, we investigated the effects of TE and TM polarized light on two nanostructures. After varying the angle of incidence of the polarized light, we find that the absorptivity of the nanostructures under TM polarized incident light is a convex function and the absorptivity under TE polarized incident light is a decreasing function. However, after calculating the absorptivity of nanostructures under mixed polarized light, we found that when the angle of the incident light is less than 20°, the light absorptivity of the GaN nanohole array can be improved, and for nanorod arrays, the angle of incidence does not exceed 40°. In summary, we conclude that GaN nanohole arrays with large hole sizes could provide high absorption performance much easier than GaN nanorod arrays, and the incidence angle less than 20° are also beneficial for improving the light trapping ability of GaN nanohole array. Therefore, the



research in this paper will provide a design direction for the realization of light absorption by UV detectors.

**Funding information** This work is supported by Qing Lan Project of Jiangsu Province-China (Grant No.2017-AD41779) and the Six Talent Peaks Project in Jiangsu Province-China (Grant No.2015-XCL-008). Qinghua Lv of Hubei University of Technology is greatly appreciated for the help of COMSOL Multiphysics Business Package calculations.

#### Compliance with ethical standards

**Conflict of interest** The authors declare that they have no conflict of interest.

**Human and animal rights and informed consent** This article does not contain any studies with human participants or animals performed by any of the authors.

#### References

- Adib MMH, Mullick TU, Khalil MI, Chowdhury AM, Chang GK, Amin N (2012) Optical absorption enhancement in slanted micro-hole C-Si for photovoltaic applications. 2012 Asia communications and photonics conference (ACP 2012) 3
- Antoine-Vincent N, Natali F, Mihailovic M, Vasson A, Leymarie J, Disseix P, Byrne D, Semond F, Massies J (2003) Determination of the refractive indices of AlN, GaN, and grown on (111) Si substrates. *J Appl Phys* 93(9):5222–5226
- Cao LY, Fan PY, Vasudev AP, White JS, Yu ZF, Cai WS, Schuller JA, Fan SH, Brongersma ML (2010) Semiconductor nanowire optical antenna solar absorbers. *Nano Lett* 10(2):439–445
- Chen TG, Yu PC, Chen SW, Chang FY, Huang BY, Cheng YC, Hsiao JC, Li CK, Wu YR (2014) Characteristics of large-scale nanohole arrays for thin-silicon photovoltaics. *Prog Photovolt* 22(4):452–461
- Cheng HB, Li J, Wu DX, Li YX, Wang ZG, Wang XY, Zheng XJ (2015) Effects of precursor-substrate distances on the growth of GaN nanowires. *J Nanomater* 343541
- Chung BC, Gershenson M (1992) The influence of oxygen on the electrical and optical properties of GaN crystals grown by metalorganic vapor phase epitaxy. *J Appl Phys* 72(2):651–659
- Deng C, Tan XY, Jiang LH, Tu YT, Ye M, Yi YS (2018) Efficient light trapping in silicon inclined nanohole arrays for photovoltaic applications. *Opt Commun* 407:199–203
- Du QG, Kam CH, Demir HV, Yu HY, Sun XW (2011) Enhanced optical absorption in nanopatterned silicon thin films with a nano-cone-hole structure for photovoltaic applications. *Opt Lett* 36(9):1713–1715
- Fang X, Zhao CY, Bao H (2014) Radiative behaviors of crystalline silicon nanowire and nanohole arrays for photovoltaic applications. *J Quant Spectrosc Radiat Transf* 133:579–588
- Fu R, Chang B, Qian Y, Qiu Y, Yang Y (2010) The research of surface state and photoelectronic emission characteristic of NEA GaN photocathode. In: Proceedings 8th International Vacuum Electron Sources Conference and Nanocarbon (2010 IVESC) 83–83
- Fu R, Wu XF, Wang XL, Ma W, Yuan L, Gao L, Huang KK, Feng SH (2018) Low-temperature hydrothermal fabrication of Fe<sub>3</sub>O<sub>4</sub> nanostructured solar selective absorption films. *Appl Surf Sci* 458:629–637
- Garnett E, Yang PD (2008) Silicon nanowire radial p-n junction solar cells. *J Am Chem Soc* 130(29):9224–9225
- Garnett E, Yang PD (2010) Light trapping in silicon nanowire solar cells. *Nano Lett* 10(3):1082–1087
- Han SE, Chen G (2010) Optical absorption enhancement in silicon nanohole arrays for solar photovoltaics. *Nano Lett* 10(3):1012–1015
- Hong L, Rusli WXC, Zheng HY, Wang H, Yu HY (2014) Design guidelines for Si (1 1 1) inclined nanohole arrays in thin-film solar cells. *IEEE Trans Nanotechnol* 13(3):431–436
- Kang SH, Fang TH (2014) Size effect on compression properties of GaN nanocones examined using in situ transmission electron microscopy. *J Alloys Compd* 597:72–78
- Kim YJ, Lee GJ, Kim S, Min JW, Jeong SY, Yoo YJ, Lee S, Song YM (2018) Efficient light absorption by GaN truncated nanocones for high performance water splitting applications. *ACS Appl Mater Interfaces* 10(34):28672–28678
- Li YH, Yan X, Wu Y, Zhang X, Ren XM (2015) Plasmon-enhanced light absorption in GaAs nanowire Array solar cells. *Nanoscale Res Lett* 10:436
- Lin H, Xiu F, Fang M, Yip S, Cheung HY, Wang FY, Han N, Chan KS, Wong CY, Ho JC (2014) Rational design of inverted nanopencil arrays for cost-effective, broadband, and omnidirectional light harvesting. *ACS Nano* 8(4):3752–3760
- Look DC, Jones RL, Sun XL, Brillson LJ, Ager JW, Park SS, Han JH, Molnar RM, Maslar JE (2002) Electrical and optical properties of GaN/Al<sub>2</sub>O<sub>3</sub> interfaces. *J Phys-Condensed Matter* 14(48):13337–13344
- Makableh YF, Al-Fandi M, Khasawneh M, Tavares CJ (2018) Comprehensive design analysis of ZnO anti-reflection nanostructures for Si solar cells. *Superlattice Microst* 124:1–9
- Peng KQ, Wang X, Li L, Wu XL, Lee ST (2010) High-performance silicon nanohole solar cells. *J Am Chem Soc* 132(20):6872–6873
- Tan XY, Yan WS, Tu YT, Deng C (2017) Small pyramidal textured ultrathin crystalline silicon solar cells with double-layer passivation. *Opt Express* 25(13):14725–14731
- Wang XL, Wu XF, Yuan L, Zhou CP, Wang YX, Huang KK, Feng SH (2016) Solar selective absorbers with foamed nanostructure prepared by hydrothermal method on stainless steel. *Sol Energy Mater Sol Cells* 146:99–106
- Wang JZ, Xu ZP, Bian F, Wang HY, Wang J (2017a) Design and analysis of light trapping in thin-film gallium arsenide solar cells using an efficient hybrid nanostructure. *J Nanophoton* 11(4):046017
- Wang XL, Wu XF, Yuan L, Huang KK, Feng SH (2017b) Ultra-low reflection CuO nanowire array in-situ grown on copper sheet. *Mater Des* 113:297–304
- Wu D, Tang XH, Wang K, He ZB, Li XQ (2017) An efficient and effective design of InP nanowires for maximal solar energy harvesting. *Nanoscale Res Lett* 12(1):604

Xu ZP, Huangfu HC, Li XW, Qiao HL, Guo WC, Guo JW, Wang HY (2016) Role of nanocone and nanohemisphere arrays in improving light trapping of thin film solar cells. *Opt Commun* 377:104–109

Xu ZP, Huangfu HC, He L, Wang JZ, Yang D, Guo JW, Wang HY (2017) Light-trapping properties of the Si inclined nanowire arrays. *Opt Commun* 382:332–336

Yoshida H, Urushido T, Miyake H, Hiramatsu K (2001) Formation of GaN self-organized nanotips by nanomasking effect. *MRS Online Proc Library Archive* 693(40):1301

**Publisher's note** Springer Nature remains neutral with regard to jurisdictional claims in published maps and institutional affiliations.